Chapter 1

Fundamentals of Finite Element Method for structural applications

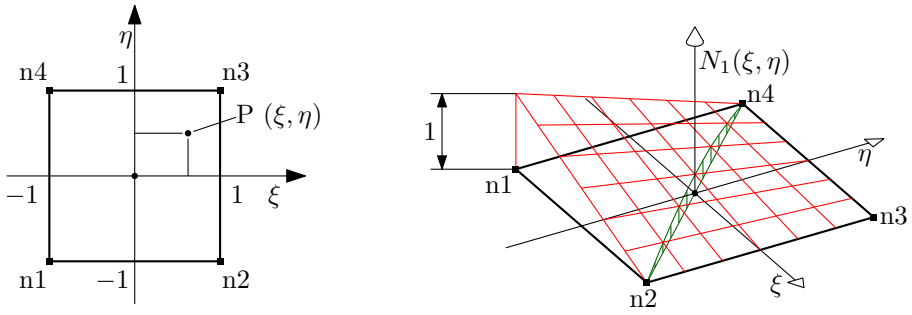

(a) (b)

Figure 1.1: Quadrilateral elementary domain (a), and a representative weight function (b).

1.1 Preliminary results

1.1.1 Interpolation functions for the quadrilateral domain

The elementary quadrilateral domain. A quadrilateral domain is considered whose vertices are conventionally located at the $(\pm 1, \pm 1)$ points of an adimensional (ξ, η) plane coordinate system, see Figure 1.1. Scalar values f_i are associated to a set of *nodal* points $\mathrm{P}_i \equiv [\xi_i, \eta_i]$, which for the present case coincide with the quadrangle vertices, numbered as in Figure.

A $f(\xi, \eta)$ interpolation function may be devised by defining a set of nodal influence functions $N_i(\xi, \eta)$ to be employed as the coefficients (weights) of a moving weighted average

$$f(\xi, \eta) \stackrel{\text{def}}{=} \sum_i N_i(\xi, \eta) f_i \tag{1.1}$$

Requisites for such weight functions are:

- the influence of a node is unitary at its location, whereas the influence of the others locally vanishes, i.e.

  $$N_i(\xi_j, \eta_j) = \delta_{ij} \tag{1.2}$$

  where δ_{ij} is the Kronecker delta function.

- for each point of the domain, the sum of the weights is unitary

$$\sum_i N_i(\xi,\eta) = 1,\ \forall[\xi,\eta] \tag{1.3}$$

Moreover, suitable functions should be continuous and straightforwardly differentiable up to any required degree.

Low order polynomials are ideal candidates for the application; for the particular domain, the nodal weight functions may be stated as

$$N_i(\xi,\eta) \stackrel{\text{def}}{=} \frac{1}{4}\left(1 \pm \xi\right)\left(1 \pm \eta\right), \tag{1.4}$$

where sign ambiguity is resolved for each i-th node by enforcing Eqn. 1.2.

The (1.3) combination of 1.4 functions turns into a general linear relation in (ξ,η) with coplanar in the ξ,η,f space – but otherwise arbitrary – nodal points.

Further generality may be introduced by *not* enforcing coplanarity.

The weight functions for the four-node quadrilateral are in fact quadratic although incomplete[1] in nature, due to the presence of the $\xi\eta$ product, and the absence of any ξ^2,η^2 term.

Each term, and the combined $f(\xi,\eta)$ function, defined as in Eqn. 1.1, behave linearly if restricted to ξ = const. or η = const. loci – namely along the four edges; quadratic behaviour may instead arise along a general direction, e.g. along the diagonals, as in Fig. 1.1b example. Such behaviour is called *bilinear*.

We now consider the $f(\xi,\eta)$ weight function partial derivatives. The partial derivative

$$\frac{\partial f}{\partial \xi} = \underbrace{\left(\frac{f_2 - f_1}{2}\right)}_{[\Delta f/\Delta\xi]_{12}} \underbrace{\left(\frac{1-\eta}{2}\right)}_{N_1+N_2} + \underbrace{\left(\frac{f_3 - f_4}{2}\right)}_{[\Delta f/\Delta\xi]_{43}} \underbrace{\left(\frac{1+\eta}{2}\right)}_{N_4+N_3} = a\eta + b \tag{1.5}$$

linearly varies from the incremental ratio value measured at the $\eta = -1$ lower edge, to the value measured at the $\eta = 1$ upper edge; the other partial derivative

$$\frac{\partial f}{\partial \eta} = \left(\frac{f_4 - f_1}{2}\right)\left(\frac{1-\xi}{2}\right) + \left(\frac{f_3 - f_2}{2}\right)\left(\frac{1+\xi}{2}\right) = c\xi + d. \tag{1.6}$$

[1] or, equivalently, *enriched linear*, as discussed above and in the following

behaves similarly, with $c = a$. However, partial derivatives in ξ, η remain constant along the corresponding differentiation direction [2].

The general quadrilateral domain. The interpolation functions introduced above for the natural quadrilateral may be profitably employed in defining a coordinate mapping between a general quadrangular domain – see Fig. 1.2a – and its reference counterpart, see Figures 1.1 and 1.2b.

In particular, we first define the $\underline{\xi}_i \mapsto \underline{\mathrm{x}}_i$ coordinate mapping for the four vertices[3] alone, where ξ, η are the reference (or natural, or elementary) coordinates and x, y are their physical counterpart.

Then, a mapping for the inner points may be derived by interpolation, namely

$$\underline{\mathrm{x}} = \underline{\mathrm{m}}\left(\underline{\xi}\right) = \sum_{i=1}^{4} N_i\left(\underline{\xi}\right) \underline{\mathrm{x}}_i \tag{1.7}$$

The availability of an inverse $\underline{\mathrm{m}}^{-1} : \underline{\mathrm{x}} \mapsto \underline{\xi}$ mapping is not granted; in particular, a closed form representation for such inverse is not generally available[4].

In the absence of an handy inverse mapping function, it is convenient to reinstate the interpolation procedure obtained for the natural domain, i.e.

$$f(\xi, \eta) \stackrel{\text{def}}{=} \sum_i N_i(\xi, \eta) f_i \tag{1.8}$$

The four f_i nodal values are interpolated based on the *natural* ξ, η coordinates of an inner P point, and not as a function of its physical x, y coordinates, that are never promoted to the independent variable role.

As already mentioned, the $\underline{\mathrm{m}}$ mapping behaves linearly along η =const. and ξ =const. one dimensional subdomains, and in particular along

[2] The relevance of such partial derivative orders will appear clearer to the reader once the strain field will have been derived in paragraph XXX.

[3] The condensed notation $\underline{\xi}_i \equiv (\xi_i, \eta_i)$, $\underline{\mathrm{x}}_i \equiv (x_i, y_i)$ for coordinate vectors is employed.

[4] Inverse relations are derived in [1], which however are case-defined and based on a selection table; for a given $\bar{\underline{\mathrm{x}}}$ physical point, however, Newton-Raphson iterations rapidly converge to the $\bar{\underline{\xi}} = \underline{\mathrm{m}}^{-1}\left(\bar{\underline{\mathrm{x}}}\right)$ solution if the centroid is chosen for algorithm initialization, see Section XXX

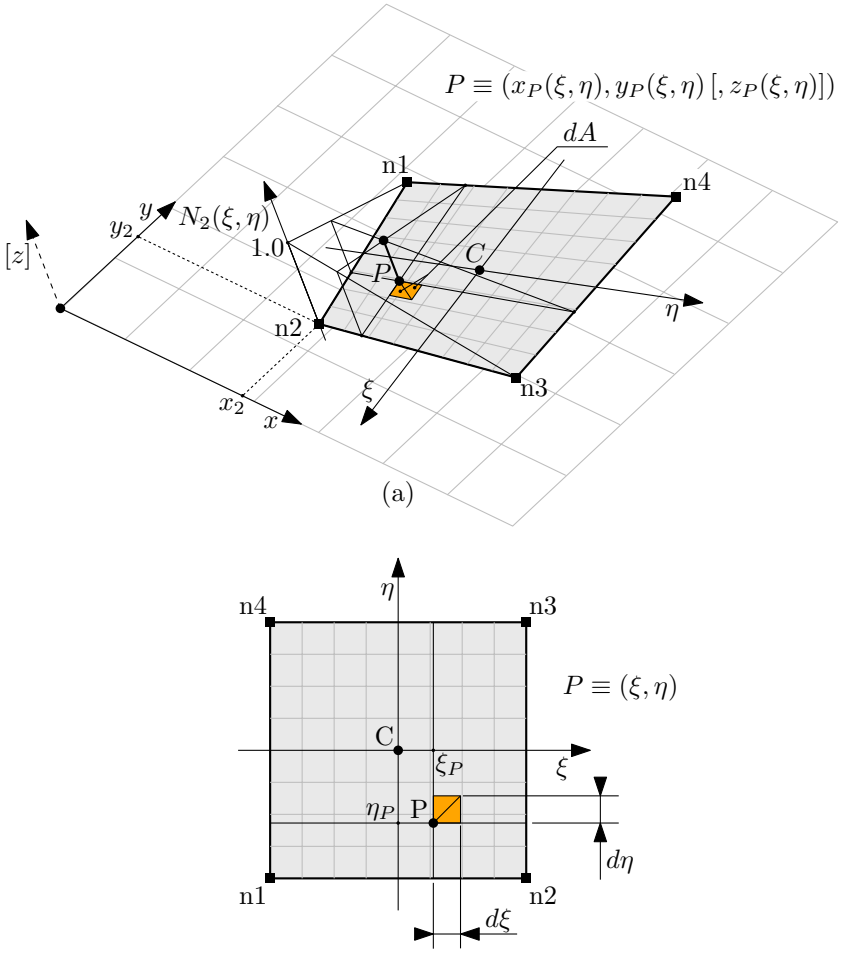

Figure 1.2: Quadrilateral general domain, (a), and its reference counterpart (b). If the general quadrangle is defined within a spatial environment, and not as a figure lying on the xy plane, limited z_i offsets are allowed at nodes with respect to such plane, which are not considered in Figure.

the quadrangle edges[5]; the inverse mapping $\underline{\mathrm{m}}^{-1}$ exists along these line segments under the further condition that their length is nonzero[6], and it is a linear function[7] . Being a composition of linear functions, the interpolation function $f(\underline{\mathrm{m}}^{-1}(x,y))$ is also linear along the aforementioned subdomains, and in particular along the quadrangle edges.

The directional derivatives of f with respect to x or y are obtained based the indirect relation

$$\begin{bmatrix} \frac{\partial f}{\partial \xi} \\ \frac{\partial f}{\partial \eta} \end{bmatrix} = \underbrace{\begin{bmatrix} \frac{\partial x}{\partial \xi} & \frac{\partial y}{\partial \xi} \\ \frac{\partial x}{\partial \eta} & \frac{\partial y}{\partial \eta} \end{bmatrix}}_{\underline{\underline{\mathrm{J}}}'(\xi,\eta)} \begin{bmatrix} \frac{\partial f}{\partial x} \\ \frac{\partial f}{\partial y} \end{bmatrix} \tag{1.9}$$

.

The function derivatives with respect to ξ, η are obtained as

$$\begin{bmatrix} \frac{\partial f}{\partial \xi} \\ \frac{\partial f}{\partial \eta} \end{bmatrix} = \sum_i \begin{bmatrix} \frac{\partial N_i}{\partial \xi} \\ \frac{\partial N_i}{\partial \eta} \end{bmatrix} f_i. \tag{1.10}$$

The *transposed* Jacobian matrix of the mapping function that appears in 1.9 is

$$\underline{\underline{\mathrm{J}}}'(\xi,\eta) = \begin{bmatrix} \frac{\partial x}{\partial \xi} & \frac{\partial y}{\partial \xi} \\ \frac{\partial x}{\partial \eta} & \frac{\partial y}{\partial \eta} \end{bmatrix} \tag{1.11}$$

$$= \sum_i \left(\begin{bmatrix} \frac{\partial N_i}{\partial \xi} & 0 \\ \frac{\partial N_i}{\partial \eta} & 0 \end{bmatrix} x_i + \begin{bmatrix} 0 & \frac{\partial N_i}{\partial \xi} \\ 0 & \frac{\partial N_i}{\partial \eta} \end{bmatrix} y_i \right) \tag{1.12}$$

If the latter matrix is assumed nonsingular – condition, this, that pairs the bijective nature of the $\underline{\mathrm{m}}$ mapping, equation 1.9 may be

[5] see paragraph XXX

[6] The case exists of an edge whose endpoints are superposed, i.e. the edge collapses to a point.

[7] A constructive proof may be defined for each edge by retrieving the non-uniform amongst the ξ, η coordinates, namely λ, as the ratio

$$\lambda = 2\frac{(x_Q - x_i)(x_j - x_i) + (y_Q - y_i)(y_j - y_i)}{(x_j - x_i)^2 + (y_j - y_i)^2} - 1,$$

where Q is a generic point along the edge, and i,j are the two subdomain endpoints at which λ equates -1 and $+1$, respectively. A similar function may be defined for any constant ξ, η segment.

inverted, thus leading to the form

$$\begin{bmatrix} \frac{\partial f}{\partial x} \\ \frac{\partial f}{\partial y} \end{bmatrix} = \left(\underline{\underline{\mathrm{J}}}' \right)^{-1} \begin{bmatrix} \dots & \frac{\partial N_i}{\partial \xi} & \dots \\ \dots & \frac{\partial N_i}{\partial \eta} & \dots \end{bmatrix} \begin{bmatrix} \vdots \\ f_i \\ \vdots \end{bmatrix}, \tag{1.13}$$

where the inner mechanics of the matrix-vector product are appointed for the Eq. 1.10 summation.

1.1.2 Gaussian quadrature rules for some relevant domains.

Reference one dimensional domain. The gaussian quadrature rule for approximating the definite integral of a $f(\xi)$ function over the $[-1, 1]$ reference interval is constructed as the customary weighted sum of internal function samples, namely

$$\int_{-1}^{1} f(\xi) d\xi \approx \sum_{i=1}^{n} f(\xi_i) w_i; \tag{1.14}$$

Its peculiarity is to employ location-weight pairs (ξ_i, w_i) that are optimal with respect to the polynomial class of functions. Nevertheless, such choice has revealed itself to be robust enough for for a more general employment.

Let's consider a m-th order polynomial

$$p(\xi) \stackrel{\text{def}}{=} a_m \xi^m + a_{m-1} \xi^{m-1} + \dots + a_1 \xi + a_0$$

whose exact integral is

$$\int_{-1}^{1} p(\xi) d\xi = \sum_{j=0}^{m} \frac{(-1)^j + 1}{j+1} a_j$$

The integration residual between the exact definite integral and the weighted sample sum is defined as

$$r\left(a_j, (\xi_i, w_i)\right) \stackrel{\text{def}}{=} \sum_{i=1}^{n} p(\xi_i) w_i - \int_{-1}^{1} p(\xi) d\xi \tag{1.15}$$

The optimality condition is stated as follows: the quadrature rule involving n sample points (ξ_i, w_i), $i = 1 \dots n$ is optimal for the m-th order polynomial if a) the integration residual is null for general

a_j values , and b) such condition does not hold for any lower-order sampling rule.

Once observed that the zero residual requirement is satisfied by any sampling rule if the polynomial a_j coefficients are all null, condition a) may be enforced by imposing that such zero residual value remains constant with varying a_j terms, i.e.

$$\begin{cases} \dfrac{\partial r\left(a_j,(\xi_i,w_i)\right)}{\partial a_j}=0, \quad j=0\dots m \end{cases} \tag{1.16}$$

A system of $m+1$ polynomial equations of degree[8] $m+1$ is hence obtained in the $2n$ (ξ_i, w_i) unknowns; in the assumed absence of redundant equations, solutions do not exist if the constraints outnumber the unknowns, i.e. $m > 2n-1$. Limiting our discussion to the threshold condition $m = 2n-1$, an attentive algebraic manipulation of Eqns. 1.16 may be performed in order to extract the (ξ_i, w_i) solutions, which are unique apart from the pair permutations[9].

Eqns. 1.16 solutions are reported in Table 1.1 for quadrature rules

[8] the $(m+1)$-th order $w_m\xi^m$ term appears in equations

[9] In this note, location-weight pairs are obtained for the gaussian quadrature rule of order $n = 2$, aiming at illustrating the general procedure. The general $m = 2n-1 = 3$rd order polynomial is stated in the form

$$p(\xi) = a_3\xi^3 + a_2\xi^2 + a_1\xi + a_0, \quad \int_{-1}^{1} p(\xi)d\xi = \frac{2}{3}a_2 + 2a_0,$$

whereas the integral residual is

$$r = a_3\left(w_1\xi_1^3 + w_2\xi_2^3\right) + a_2\left(w_1\xi_1^2 + w_2\xi_2^2 - \frac{2}{3}\right) + a_1\left(w_1\xi_1 + w_2\xi_2\right) + a_0\left(w_1 + w_2 - 2\right)$$

Eqns 1.16 may be derived as

$$\begin{cases} 0 = \frac{\partial r}{\partial a_3} = w_1\xi_1^3 + w_2\xi_2^3 & (e_1) \\ 0 = \frac{\partial r}{\partial a_2} = w_1\xi_1^2 + w_2\xi_2^2 - \frac{2}{3} & (e_2) \\ 0 = \frac{\partial r}{\partial a_1} = w_1\xi_1 + w_2\xi_2 & (e_3) \\ 0 = \frac{\partial r}{\partial a_0} = w_1 + w_2 - 2 & (e_4) \end{cases}$$

which are independent of the a_j coefficients.

By composing $\left(e_1 - \xi_1^2 e_3\right)/(w_2\xi_2)$ it is obtained that $\xi_2^2 = \xi_1^2$; e_2 may then be written as $(w_1 + w_2)\xi_1^2 = 2/3$, and then as $2\xi_1^2 = 2/3$, according to e_4. It derives that $\xi_{1,2} = \pm 1/\sqrt{3}$. Due to the opposite nature of the roots, e_3 implies $w_2 = w_1$, relation, this, that turns e_4 into $2w_1 = 2w_2 = 2$, and hence $w_{1,2} = 1$.

n	ξ_i	w_i
1	0	2
2	$\pm\frac{1}{\sqrt{3}}$	1
3	0 $\pm\sqrt{\frac{3}{5}}$	$\frac{8}{9}$ $\frac{5}{9}$
4	$\pm\sqrt{\frac{3}{7}-\frac{2}{7}\sqrt{\frac{6}{5}}}$ $\pm\sqrt{\frac{3}{7}+\frac{2}{7}\sqrt{\frac{6}{5}}}$	$\frac{18+\sqrt{30}}{36}$ $\frac{18-\sqrt{30}}{36}$

Table 1.1: Integration points for the lower order gaussian quadrature rules.

with up to $n = 4$ sample points[10].

It is noted that the integration points are symmetrically distributed with respect to the origin, and that the function is never sampled at the $\{-1, 1\}$ extremal points.

General one dimensional domain. The extension of the one dimensional quadrature rule from the reference domain $[-1, 1]$ to a general $[a, b]$ domain is pretty straightforward, requiring just a change of integration variable to obtain the following

$$\begin{aligned}\int_a^b f(x)dx &= \frac{b-a}{2}\int_{-1}^{1} f\left(\frac{b+a}{2}+\frac{b-a}{2}\xi\right)d\xi,\\ &\approx \frac{b-a}{2}\sum_{i=1}^{n} f\left(\frac{b+a}{2}+\frac{b-a}{2}\xi_i\right)w_i.\end{aligned}$$

Reference quadrangular domain. A quadrature rule for the reference quadrangular domain of Figure 1.1a may be derived by nesting the quadrature rule defined for the reference interval, see Eqn. 1.14, thus obtaining

$$\int_{-1}^{1}\int_{-1}^{1} f(\xi,\eta)\,d\xi d\eta \approx \sum_{i=1}^{p}\sum_{j=1}^{q} f\left(\xi_i,\eta_j\right)w_i w_j \tag{1.17}$$

[10] see `https://pomax.github.io/bezierinfo/legendre-gauss.html` for higher order gaussian quadrature rule sample points.

where (ξ_i, w_i) and (η_j, w_j) are the coordinate-weight pairs of the two quadrature rules of p and q order, respectively, employed for spanning the two coordinate axes. The equivalent notation

$$\int_{-1}^{1}\int_{-1}^{1} f(\xi,\eta)\, d\xi d\eta \approx \sum_{l=1}^{pq} f\left(\underline{\xi}_l\right) w_l \tag{1.18}$$

emphasises the characteristic nature of the pq point/weight pairs for the domain and for the quadrature rule employed; a general integer bijection[11] $\{1 \dots pq\} \leftrightarrow \{1 \dots p\} \times \{1 \dots q\}$, $l \leftrightarrow (i,j)$ may be utilized to formally derive the two-dimensional quadrature rule pairs

$$\underline{\xi}_l = \left(\xi_i, \eta_j\right), \quad w_l = w_i w_j, \quad l = 1 \dots pq \tag{1.19}$$

from their uniaxial counterparts.

General quadrangular domain. The rectangular infinitesimal area $dA_{\xi\eta} = d\xi d\eta$ in the neighborhood of a ξ_P, η_P location, see Figure 1.2b, is mapped to the quadrangle of Figure 1.2a, which is composed by the two triangular areas

$$\begin{aligned} dA_{xy} = \quad & \frac{1}{2!}\begin{vmatrix} 1 & x(\xi_P, \eta_P) & y(\xi_P, \eta_P) \\ 1 & x(\xi_P + d\xi, \eta_P) & y(\xi_P + d\xi, \eta_P) \\ 1 & x(\xi_P, \eta_P + d\eta) & y(\xi_P, \eta_P + d\eta) \end{vmatrix} + \\ & + \frac{1}{2!}\begin{vmatrix} 1 & x(\xi_P + d\xi, \eta_P + d\eta) & y(\xi_P + d\xi, \eta_P + d\eta) \\ 1 & x(\xi_P, \eta_P + d\eta) & y(\xi_P, \eta_P + d\eta) \\ 1 & x(\xi_P + d\xi, \eta_P) & y(\xi_P + d\xi, \eta_P) \end{vmatrix}. \end{aligned} \tag{1.20}$$

[11] e.g.

$$\{i-1; j-1\} = (l-1) \bmod (p,q), \quad l - 1 = (j-1)q + (i-1)$$

where the operator

$$\{a_n; \dots; a_3; a_2; a_1\} = m \bmod (b_n, \dots, b_3, b_2, b_1)$$

consists in the extraction of the n least significant a_i digits of a mixed radix representation of the integer m with respect to the sequence of b_i bases, with $i = 1 \dots n$.

The determinant formula for the area of a triangle, shown below along with its n-dimensional symplex hypervolume generalization,

$$\mathcal{A} = \frac{1}{2!}\begin{vmatrix} 1 & x_1 & y_1 \\ 1 & x_2 & y_2 \\ 1 & x_3 & y_3 \end{vmatrix}, \quad \mathcal{H} = \frac{1}{n!}\begin{vmatrix} 1 & \underline{\mathrm{x}}_1 \\ 1 & \underline{\mathrm{x}}_2 \\ \vdots & \vdots \\ 1 & \underline{\mathrm{x}}_{n+1} \end{vmatrix} \tag{1.21}$$

has been employed above.

By operating a local multivariate linearization of the 1.20 matrix terms, the relation

$$\begin{aligned} dA_{xy} \approx \quad & \frac{1}{2!}\begin{vmatrix} 1 & x & y \\ 1 & x + x_{,\xi} d\xi & y + y_{,\xi} d\xi \\ 1 & x + x_{,\eta} d\eta & y + y_{,\eta} d\eta \end{vmatrix} + \\ & + \frac{1}{2!}\begin{vmatrix} 1 & x + x_{,\xi} d\xi + x_{,\eta} d\eta & y + y_{,\xi} d\xi + y_{,\eta} d\eta \\ 1 & x + x_{,\eta} d\eta & y + y_{,\eta} d\eta \\ 1 & x + x_{,\xi} d\xi & y + y_{,\xi} d\xi \end{vmatrix} \end{aligned}$$

is obtained, where $x, y, x_{,\xi}, x_{,\eta}, y_{,\xi}$, and $y_{,\eta}$ are the x, y functions and their first order partial derivatives, sampled at the (ξ_P, η_P) point; infinitesimal terms of order higher than $d\xi, d\eta$ are neglected.

After some matrix manipulations[12], the following expression is obtained

$$dA_{xy} = \begin{vmatrix} 1 & 0 & 0 \\ 0 & x_{,\xi} & y_{,\xi} \\ 0 & x_{,\eta} & y_{,\eta} \end{vmatrix} d\xi d\eta = \underbrace{\begin{vmatrix} x_{,\xi} & y_{,\xi} \\ x_{,\eta} & y_{,\eta} \end{vmatrix}}_{|J^{\mathrm{T}}(\xi_P, \eta_P)|} dA_{\xi\eta} \tag{1.22}$$

that equates the ratio of the mapped and of the reference areas to the determinant of the transformation (transpose) Jacobian matrix[13].

[12] For both the determinants, the first column is multiplied by x_P and subtracted to the second column, and then subtracted to the third column once multiplied by y_P. The first row is then subtracted to the others. On the second determinant alone, both the second and the third columns are changed in sign; then, the second and the third rows are summed to the first. The two determinants are now formally equal, and the two 1/2 multipliers are summed to provide unity. The $d\xi$ and the $d\eta$ factors may then be collected from the second and the third rows, respectively.

[13] The Jacobian matrix for a general $\underline{\xi} \mapsto \underline{\mathrm{x}}$ mapping is in fact defined according to

$$[J(\underline{\xi}_P)]_{ij} \stackrel{\text{def}}{=} \left.\frac{\partial x_i}{\partial \xi_j}\right|_{\underline{\xi} = \underline{\xi}_P} \qquad i, j = 1 \dots n$$

being i the generic matrix term row index, and j the column index

After the preparatory passages above, we obtain

$$\iint_{A_{xy}} g(x,y)dA_{xy} = \iint_{-1}^{1} g\left(x\left(\xi,\eta\right), y\left(\xi,\eta\right)\right)\left|J(\xi,\eta)\right| d\xi d\eta, \qquad (1.23)$$

thus reducing the quadrature over a general domain to its reference domain counterpart, which has been discussed in the paragraph above.

Based on Eqn. 1.18, the quadrature rule

$$\iint_{A_{xy}} g(\underline{\mathrm{x}})dA_{xy} \approx \sum_{l=1}^{pq} g\left(\underline{\mathrm{x}}\left(\underline{\xi}_l\right)\right)\left|J(\underline{\xi}_l)\right| w_l \qquad (1.24)$$

is derived, stating that the definite integral of a g integrand over a quadrangular domain pertaining to the physical x, y plane (x, y are dimensional quantities, namely lengths) may be approximated as follows:

1. a reference-to-physical domain mapping is defined, that is based on the vertex physical coordinate interpolation;

2. the function is sampled at the physical locations that are the images of the Gaussian integration points previously obtained for the reference domain;

3. a weighted sum of the collected samples is performed, where the weights consist in the product of i) the adimensional w_l Gauss point weight (suitable for integrating on the reference domain), and ii) a dimensional area scaling term, that equals the determinant of the transformation Jacobian matrix, locally evaluated at the Gauss points.

1.2 Basic theory of plates

P displacement components as a function of the Q reference point motion.

$$u_P = u + z\,(1 + \tilde{\epsilon}_z)\,sin\,\varphi \tag{1.25}$$
$$v_P = v - z\,(1 + \tilde{\epsilon}_z)\,sin\,\theta \tag{1.26}$$
$$w_P = w + z\,((1 + \tilde{\epsilon}_z)\,cos(\varphi)\,cos(\theta) - 1) \tag{1.27}$$

$$\tilde{\epsilon}(z) = \frac{1}{z}\int_0^z \epsilon_z d\varsigma \tag{1.28}$$
$$= \frac{1}{z}\int_0^z \left(-\nu\epsilon_x - \nu\epsilon_y\right) d\varsigma \tag{1.29}$$

P displacement components as a function of the Q reference point motion, linarized with respect to the small rotations and small strain hypotheses.

$$u_P = u + z\varphi \tag{1.30}$$
$$v_P = v - z\theta \tag{1.31}$$
$$w_P = w \tag{1.32}$$

Relation between the normal displacement x, y gradient (i.e. the deformed plate slope), the rotations and the out-of-plane, interlaminar, averaged shear strain components.

$$\frac{\partial w}{\partial x} = \bar{\gamma}_{zx} - \varphi \tag{1.33}$$
$$\frac{\partial w}{\partial y} = \bar{\gamma}_{yz} + \theta \tag{1.34}$$

Strains at point P.

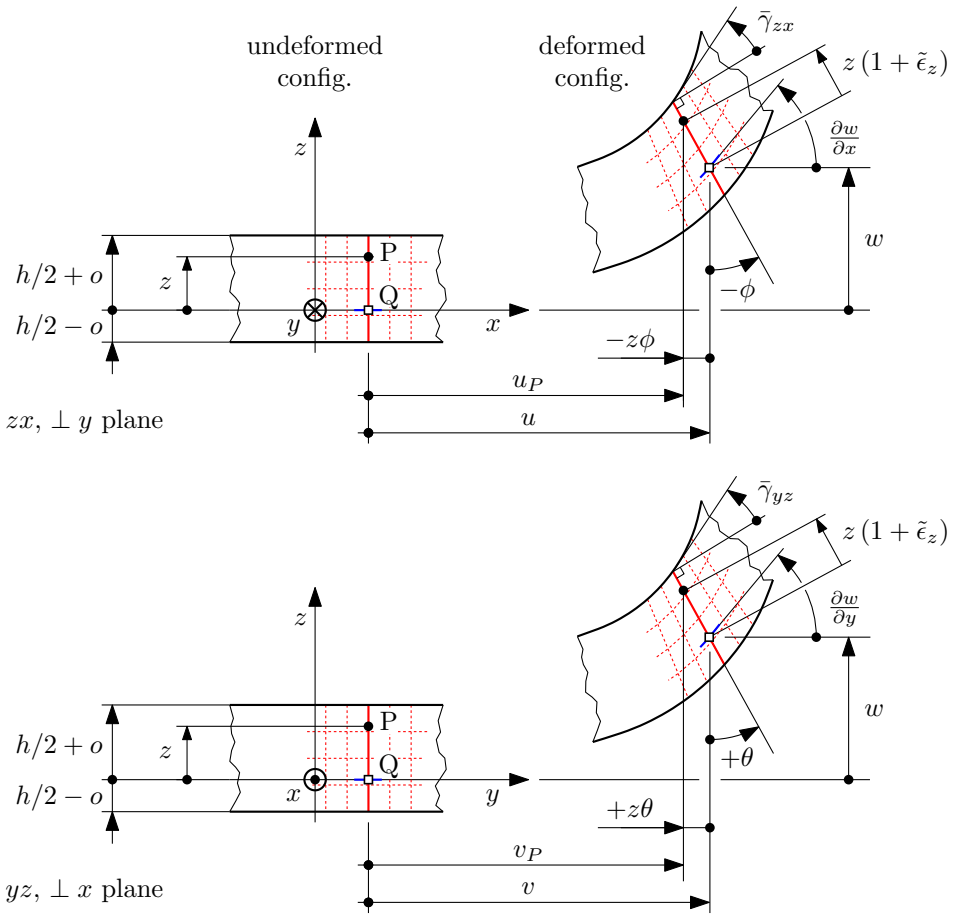

Figure 1.3: Relevant dimensions for describing the deformable plate kinematics.

$$\epsilon_x = \frac{\partial u_P}{\partial x} = \frac{\partial u}{\partial x} + z\frac{\partial \varphi}{\partial x} \tag{1.35}$$

$$\epsilon_y = \frac{\partial v_P}{\partial y} = \frac{\partial v}{\partial y} - z\frac{\partial \theta}{\partial y} \tag{1.36}$$

$$\gamma_{xy} = \frac{\partial u_P}{\partial y} + \frac{\partial v_P}{\partial x} \tag{1.37}$$

$$= \left(\frac{\partial u}{\partial y} + \frac{\partial v}{\partial x}\right) + z\left(+\frac{\partial \varphi}{\partial y} - \frac{\partial \theta}{\partial x}\right) \tag{1.38}$$

Generalized plate strains: membrane strains.

$$\underline{\bar{\epsilon}} = \begin{pmatrix} \frac{\partial u}{\partial x} \\ \frac{\partial v}{\partial y} \\ \frac{\partial u}{\partial y} + \frac{\partial v}{\partial x} \end{pmatrix} = \begin{pmatrix} \bar{\epsilon}_x \\ \bar{\epsilon}_y \\ \bar{\gamma}_{xy} \end{pmatrix} \tag{1.39}$$

Generalized plate strains: curvatures.

$$\underline{\kappa} = \begin{pmatrix} +\frac{\partial \varphi}{\partial x} \\ -\frac{\partial \theta}{\partial y} \\ +\frac{\partial \varphi}{\partial y} - \frac{\partial \theta}{\partial x} \end{pmatrix} = \begin{pmatrix} \kappa_x \\ \kappa_y \\ \kappa_{xy} \end{pmatrix} \tag{1.40}$$

Compact form for the strain components at P.

$$\underline{\epsilon} = \underline{\bar{\epsilon}} + z\,\underline{\kappa} \tag{1.41}$$

Hook law for an isotropic material, under plane stress conditions.

$$\underline{\underline{\mathrm{D}}} = \frac{E}{1-\nu^2}\begin{pmatrix} 1 & \nu & 0 \\ \nu & 1 & 0 \\ 0 & 0 & \frac{1-\nu}{2} \end{pmatrix} \tag{1.42}$$

Normal components for stress and strain, the latter for the isotropic material case only.

$$\sigma_z = 0 \tag{1.43}$$

$$\epsilon_z = -\nu\left(\epsilon_x + \epsilon_y\right) \tag{1.44}$$

Stresses at P.

$$\underline{\sigma} = \underline{\underline{\mathrm{D}}}\,\underline{\epsilon} = \underline{\underline{\mathrm{D}}}\,\underline{\bar{\epsilon}} + z\,\underline{\underline{\mathrm{D}}}\,\underline{\kappa} \tag{1.45}$$

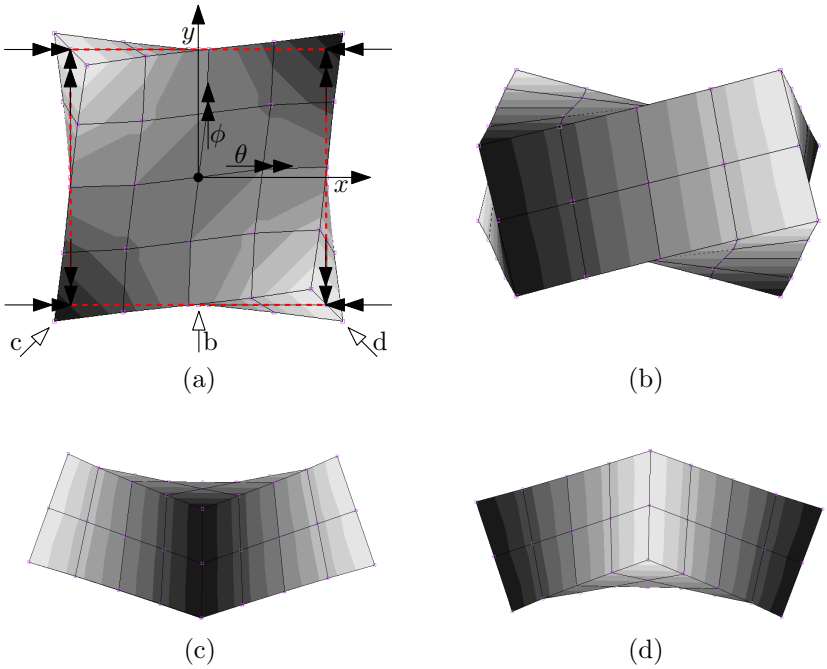

Figure 1.4: Positive κ_{xy} torsional curvature for the plate element. Subfigure (a) shows the positive γ_{xy} shear strain at the upper surface, the (in-plane) undeformed midsurface, and the negative γ_{xy} at the lower surface; the point of sight related to subfigures (b) to (d) are also evidenced. θ and φ rotation components decrease with x and increase with y, respectively, thus leading to positive κ_{xy} contributions. As shown in subfigures (c) and (d), the torsional curvature of subfigure (b) evolves into two anticlastic bending curvatures if the reference system is aligned with the square plate element diagonals, and hence rotated by 45° with respect to z.

Membrane (direct and shear) stress resultants (stress flows).

$$\underline{\mathrm{q}} = \begin{pmatrix} q_x \\ q_y \\ q_{xy} \end{pmatrix} = \int_h \underline{\sigma}\, dz \tag{1.46}$$

$$= \underbrace{\int_h \underline{\underline{\mathrm{D}}}\, dz}_{\underline{\underline{\mathrm{A}}}}\, \underline{\bar{\epsilon}} + \underbrace{\int_h \underline{\underline{\mathrm{D}}}\, z dz}_{\underline{\underline{\mathrm{B}}}}\, \underline{\kappa} \tag{1.47}$$

Bending and torsional moment stress resultants (moment flows).

$$\underline{\mathrm{m}} = \begin{pmatrix} m_x \\ m_y \\ m_{xy} \end{pmatrix} = \int_h \underline{\sigma}\, dz \tag{1.48}$$

$$= \underbrace{\int_h \underline{\underline{\mathrm{D}}}\, z dz}_{\underline{\underline{\mathrm{B}}} \equiv \underline{\underline{\mathrm{B}}}^{\mathrm{T}}}\, \underline{\bar{\epsilon}} + \underbrace{\int_h \underline{\underline{\mathrm{D}}}\, z^2 dz}_{\underline{\underline{\mathrm{C}}}}\, \underline{\kappa} \tag{1.49}$$

Cumulative generalized strain - stress relations for the plate (or for the laminate)

$$\begin{pmatrix} \underline{\mathrm{q}} \\ \underline{\mathrm{m}} \end{pmatrix} = \begin{pmatrix} \underline{\underline{\mathrm{A}}} & \underline{\underline{\mathrm{B}}} \\ \underline{\underline{\mathrm{B}}}^{\mathrm{T}} & \underline{\underline{\mathrm{C}}} \end{pmatrix} \begin{pmatrix} \underline{\bar{\epsilon}} \\ \underline{\kappa} \end{pmatrix} \tag{1.50}$$

Hook law for the orthotropic material in plane stress conditions, with respect to principal axes of orthotropy;

$$\underline{\underline{\mathrm{D}}}_{123} = \begin{pmatrix} \frac{E_1}{1-\nu_{12}\nu_{21}} & \frac{\nu_{21}E_1}{1-\nu_{12}\nu_{21}} & 0 \\ \frac{\nu_{12}E_2}{1-\nu_{12}\nu_{21}} & \frac{E_2}{1-\nu_{12}\nu_{21}} & 0 \\ 0 & 0 & G_{12} \end{pmatrix} \tag{1.51}$$

$$\begin{pmatrix} \sigma_1 \\ \sigma_2 \\ \tau_{12} \end{pmatrix} = \underline{\underline{\mathrm{T}}}_1 \begin{pmatrix} \sigma_x \\ \sigma_y \\ \tau_{xy} \end{pmatrix} \qquad \begin{pmatrix} \epsilon_1 \\ \epsilon_2 \\ \gamma_{12} \end{pmatrix} = \underline{\underline{\mathrm{T}}}_2 \begin{pmatrix} \epsilon_x \\ \epsilon_y \\ \gamma_{xy} \end{pmatrix} \tag{1.52}$$

where

$$\underline{\underline{\mathrm{T}}}_1 = \begin{pmatrix} m^2 & n^2 & 2mn \\ n^2 & m^2 & -2mn \\ -mn & mn & m^2 - n^2 \end{pmatrix} \tag{1.53}$$

$$\underline{\underline{\mathrm{T}}}_2 = \begin{pmatrix} m^2 & n^2 & mn \\ n^2 & m^2 & -mn \\ -2mn & 2mn & m^2 - n^2 \end{pmatrix} \tag{1.54}$$

α is the angle between 1 and x;

$$m = cos(\alpha) \qquad\qquad n = sin(\alpha) \tag{1.55}$$

The inverse transformations may be obtained based on the relations

$$\underline{\underline{\mathrm{T}}}_1^{-1}(+\alpha) = \underline{\underline{\mathrm{T}}}_1(-\alpha) \qquad \underline{\underline{\mathrm{T}}}_2^{-1}(+\alpha) = \underline{\underline{\mathrm{T}}}_2(-\alpha) \tag{1.56}$$

Finally

$$\underline{\sigma} = \underline{\underline{\mathrm{D}}}\,\underline{\epsilon} \qquad \underline{\underline{\mathrm{D}}} \equiv \underline{\underline{\mathrm{D}}}_{xyz} = \underline{\underline{\mathrm{T}}}_1^{-1}\,\underline{\underline{\mathrm{D}}}_{123}\,\underline{\underline{\mathrm{T}}}_2 \tag{1.57}$$

Notes:

- Midplane is ill-defined if the material distribution is not symmetric; the geometric midplane (i.e. the one obtained by ignoring the material distribution) exhibits no relevant properties in general. Its definition is nevertheless pretty straighforward.
- If the unsimmetric laminate is composed by isotropic layers, a reference plane may be obtained for which the $\underline{\underline{\mathrm{B}}}$ membrane-to-bending coupling matrix vanishes; a similar condition may not be verified in the presence of orthotropic layers.
- Thermally induced distortion is not self-compensated in an unsymmetric laminate even if the temperature is held constant through the thickness.

1.3 The bilinear isoparametric shear-deformable shell element

> This is a four-node, thick-shell element with global displacements and rotations as degrees of freedom. Bilinear interpolation is used for the coordinates, displacements and the rotations. The membrane strains are obtained from the displacement field; the curvatures from the rotation field. The transverse shear strains are calculated at the middle of the edges and interpolated to the integration points. In this way, a very efficient and simple element is obtained which exhibits correct behavior in the limiting case of thin shells. The element can be used in curved shell analysis as well as in the analysis of complicated plate structures. For the latter case, the element is easy to use since connections between intersecting plates can be modeled without tying. Due to its simple formulation when compared to the standard higher order shell elements, it is less expensive and, therefore, very attractive in nonlinear analysis. The element is not very sensitive to distortion, particularly if the corner nodes lie in the same plane. All constitutive relations can be used with this element.
>
> — MSC.Marc 2013.1 Documentation, vol. B, Element library.

1.3.1 Element geometry

Once recalled the required algebraic paraphernalia, the definition of a bilinear quadrilateral shear-deformable isoparametric shell element is straightforward.

The quadrilateral element geometry is defined by the position in space of its four vertices, which constitute the set of *nodal points*, or *nodes*, i.e. the set of locations at which field components are primarily, parametrically, defined; interpolation is employed in deriving the field values elsewhere.

A suitable interpolation scheme, named *bilinear*, has been introduced in paragraph 1.1.1; the related functions depend on the normalized coordinate pair $\xi, \eta \in [-1, 1]$ that spans the elementary quadrilateral of Figure 1.1.

A global reference system OXYZ is employed for concurrently dealing with multiple elements (i.e. at a whole model scale); a more convenient, local Cxyz reference system, z being locally normal to the shell, is used when a single element is under scrutiny – e.g. in the current paragraph.

Nodal coordinates define the element initial, undeformed, geometry[14] of the portion of shell reference surface pertaining to the currente element; spatial coordinates for each other element point may be retrieved by interpolation based on the associated pair of natural ξ, η coordinates.

In particular, the C centroid is the image within the physical space of the $\xi = 0, \eta = 0$ natural coordinate system origin.

The in-plane orientation of the local Cxyz reference system is somewhat arbitrary and implementation-specific; the MSC.Marc approach is used as an example, and it is described in the following. The in-plane x, y axes are tentatively defined[15] based on the physical directions that are associated with the ξ, η natural axes, i.e. the oriented segments spanning a) from the midpoint of the n4-n1 edge to the midpoint of the n2-n3 edge, and b) from the midpoint of the n1-n2 edge to the midpoint of the n3-n4 edge, respectively; however, these two tentative axes are not mutually orthogonal in general. The mutual Cxy angle is then amended by rotating those interim axes with respect to a third, binormal axis Cz, while preserving their initial bisectrix.

The resulting quadrilateral shell element is in fact initially flat, apart from a (suggestedly limited) anticlastic curvature of the element diagonals, that is associated to the quadratic $\xi\eta$ term of the interpolation functions. The curve nature of a thin wall midsurface is thus represented by recurring to a plurality of basically flat, but mutually angled elements.

[14] They are however continuosly updated within most common nonlinear analysis frameworks, where *initial* usually refers to the last computed, aka *previous* step of an iterative scheme.

[15] The MSC.Marc element library documentation defines them as a normalized form of the

$$\left(\frac{\partial X}{\partial \xi}, \frac{\partial Y}{\partial \xi}, \frac{\partial Z}{\partial \xi}, \right)\Big|_{\xi=0,\eta=0}, \left(\frac{\partial X}{\partial \eta}, \frac{\partial Y}{\partial \eta}, \frac{\partial Z}{\partial \eta}, \right)\Big|_{\xi=0,\eta=0},$$

vectors, which are evaluated at the centroid. The two definitions may be proved equivalent based on the bilinear interpolation properties.

1.3.2 Displacement and rotation fields

The element degrees of freedom consist in the displacements and the rotations of the four quadrilateral vertices, i.e. *nodes*.

By interpolating the nodal values, displacement and rotation functions may be derived along the element as

$$\begin{bmatrix} u(\xi,\eta) \\ v(\xi,\eta) \\ w(\xi,\eta) \end{bmatrix} = \sum_{i=1}^{4} N_i(\xi,\eta) \begin{bmatrix} u_i \\ v_i \\ w_i \end{bmatrix} \tag{1.58}$$

$$\begin{bmatrix} \theta(\xi,\eta) \\ \varphi(\xi,\eta) \\ \psi(\xi,\eta) \end{bmatrix} = \sum_{i=1}^{4} N_i(\xi,\eta) \begin{bmatrix} \theta_i \\ \varphi_i \\ \psi_i \end{bmatrix} \tag{1.59}$$

with $i = 1 \dots 4$ cycling along the element nodes.

1.3.3 Strains

By recalling Eqn. 1.13, we have e.g.

$$\begin{bmatrix} \frac{\partial u}{\partial x} \\ \frac{\partial u}{\partial y} \end{bmatrix} = \underbrace{\left(\underline{\underline{\mathrm{J}}}'\right)^{-1} \begin{bmatrix} \dots & \frac{\partial N_i}{\partial \xi} & \dots \\ \dots & \frac{\partial N_i}{\partial \eta} & \dots \end{bmatrix}}_{\underline{\underline{\mathrm{L}}}(\xi,\eta)} \begin{bmatrix} \vdots \\ u_i \\ \vdots \end{bmatrix} \tag{1.60}$$

for the x-oriented displacement component; the isoparametric differential operator $\underline{\underline{\mathrm{L}}}(\xi,\eta)$ is also defined that extract the x, y directional derivatives from the nodal values of a given field component.

We now collect within the five column vectors

$$\underline{\mathrm{u}} = \begin{bmatrix} \vdots \\ u_i \\ \vdots \end{bmatrix}, \ \underline{\mathrm{v}} = \begin{bmatrix} \vdots \\ v_i \\ \vdots \end{bmatrix}, \ \underline{\mathrm{w}} = \begin{bmatrix} \vdots \\ w_i \\ \vdots \end{bmatrix}, \ \underline{\theta} = \begin{bmatrix} \vdots \\ \theta_i \\ \vdots \end{bmatrix}, \ \underline{\varphi} = \begin{bmatrix} \vdots \\ \varphi_i \\ \vdots \end{bmatrix} \tag{1.61}$$

the nodal degrees of freedom; the $\underline{\psi}$ vector associated with the drilling degree of freedom is omitted.

A block defined $Q(\xi,\eta)$ matrix is thus obtained that cumulatively relates the in-plane displacement component derivatives to the associ-

ated nodal values

$$\begin{bmatrix} \frac{\partial u}{\partial x} \\ \frac{\partial u}{\partial y} \\ \frac{\partial v}{\partial x} \\ \frac{\partial v}{\partial y} \end{bmatrix} = \underbrace{\begin{bmatrix} \underline{\underline{\mathrm{L}}}\,(\xi,\eta) & \underline{\underline{0}} \\ \underline{\underline{0}} & \underline{\underline{\mathrm{L}}}\,(\xi,\eta) \end{bmatrix}}_{\underline{\underline{\mathrm{Q}}}\,(\xi,\eta)} \begin{bmatrix} \underline{\mathrm{u}} \\ \underline{\mathrm{v}} \end{bmatrix} \tag{1.62}$$

An equivalent relation may then be obtained for the rotation field

$$\begin{bmatrix} \frac{\partial \theta}{\partial x} \\ \frac{\partial \theta}{\partial y} \\ \frac{\partial \varphi}{\partial x} \\ \frac{\partial \varphi}{\partial y} \end{bmatrix} = \underline{\underline{\mathrm{Q}}}\,(\xi,\eta) \begin{bmatrix} \underline{\theta} \\ \underline{\varphi} \end{bmatrix} \tag{1.63}$$

By making use of two auxiliary matrices $H^{\dagger}$ and $H^{\ddagger}$ that collect the $\{0, \pm 1\}$ coefficients in Eqns. 1.39 and 1.40, we obtain

$$\begin{bmatrix} \bar{\epsilon}_x \\ \bar{\epsilon}_y \\ \bar{\gamma}_{xy} \end{bmatrix} = \underbrace{\begin{bmatrix} +1 & 0 & 0 & 0 \\ 0 & 0 & 0 & +1 \\ 0 & +1 & +1 & 0 \end{bmatrix}}_{\underline{\underline{\mathrm{H}}}^{\dagger}} \begin{bmatrix} \frac{\partial u}{\partial x} \\ \frac{\partial u}{\partial y} \\ \frac{\partial v}{\partial x} \\ \frac{\partial v}{\partial y} \end{bmatrix} = \underline{\underline{\mathrm{H}}}^{\dagger}\, \underline{\underline{\mathrm{Q}}}\,(\xi,\eta) \begin{bmatrix} \underline{\mathrm{u}} \\ \underline{\mathrm{v}} \end{bmatrix} \tag{1.64}$$

$$\begin{bmatrix} \kappa_x \\ \kappa_y \\ \kappa_{xy} \end{bmatrix} = \underbrace{\begin{bmatrix} 0 & 0 & +1 & 0 \\ 0 & -1 & 0 & 0 \\ -1 & 0 & 0 & +1 \end{bmatrix}}_{\underline{\underline{\mathrm{H}}}^{\ddagger}} \begin{bmatrix} \frac{\partial \theta}{\partial x} \\ \frac{\partial \theta}{\partial y} \\ \frac{\partial \varphi}{\partial x} \\ \frac{\partial \varphi}{\partial y} \end{bmatrix} = \underline{\underline{\mathrm{H}}}^{\ddagger}\, \underline{\underline{\mathrm{Q}}}\,(\xi,\eta) \begin{bmatrix} \underline{\theta} \\ \underline{\varphi} \end{bmatrix} \tag{1.65}$$

The in plane strain tensor at each ξ, η, z point along the element may then be derived according to Eqn. 1.41 as a (linear) function of the nodal degrees of freedom

$$\underline{\epsilon}\,(\xi,\eta,z) = \begin{bmatrix} \underline{\underline{\mathrm{H}}}^{\dagger}\, \underline{\underline{\mathrm{Q}}}\,(\xi,\eta) & \underline{\underline{0}} & z\,\underline{\underline{\mathrm{H}}}^{\ddagger}\, \underline{\underline{\mathrm{Q}}}\,(\xi,\eta) \end{bmatrix} \begin{bmatrix} \underline{\mathrm{u}} \\ \underline{\mathrm{v}} \\ \underline{\mathrm{w}} \\ \underline{\theta} \\ \underline{\varphi} \end{bmatrix} \tag{1.66}$$

where the transformation matrix is block-defined by appending to the 3x8 block introduced in Eqn. 1.64 a 3x3 zero block (the $\underline{\mathrm{w}}$ out-of-plane displacements have no influence on the in-plane strain components), and then the 3x8 block presented in Eqn. 1.65.

By separating the terms of the above matrix based on their order with respect to z, we finally have.

$$\underline{\epsilon}\,(\xi,\eta,z) = \left(\underline{\underline{\mathrm{B}}}_0(\xi,\eta) + \underline{\underline{\mathrm{B}}}_1(\xi,\eta)z\right)\,\underline{\mathrm{d}} \tag{1.67}$$

The out-of-plane shear strain components, as defined in Eqns. 1.33 and 1.34, become

$$\begin{bmatrix}\bar{\gamma}_{zx}\\ \bar{\gamma}_{yz}\end{bmatrix} = \underline{\underline{\mathrm{L}}}\,(\xi,\eta)\,\underline{\mathrm{w}} + \begin{bmatrix}0 & +\underline{\underline{\mathrm{N}}}\,(\xi,\eta)\\ -\underline{\underline{\mathrm{N}}}\,(\xi,\eta) & 0\end{bmatrix}\begin{bmatrix}\underline{\theta}\\ \underline{\varphi}\end{bmatrix}, \tag{1.68}$$

and thus, by employing a notation consistent with 1.67,

$$\begin{bmatrix}\bar{\gamma}_{zx}\\ \bar{\gamma}_{yz}\end{bmatrix} = \underbrace{\begin{bmatrix}\underline{\underline{0}} & \underline{\underline{0}} & \underline{\underline{\mathrm{L}}}\,(\xi,\eta) & 0 & \underline{\underline{\mathrm{N}}}\,(\xi,\eta)\\ \underline{\underline{0}} & \underline{\underline{0}} & \underline{\underline{\mathrm{L}}}\,(\xi,\eta) & -\underline{\underline{\mathrm{N}}}\,(\xi,\eta) & 0\end{bmatrix}}_{\underline{\underline{\mathrm{B}}}_{\bar{\gamma}}(\xi,\eta)}\,\underline{\mathrm{d}} \tag{1.69}$$

where the transformation matrix that derives the out-of-plane, interlaminar strains from the nodal degrees of freedom vector is constituted by five 2×4 blocks.

1.3.4 Stresses

The plane stress relations discussed in Paragraph 1.2, see Eqns. 1.43, may be employed in deriving the in-plane stress components from the associated strains.

The G_{zx}, G_{yz} material shear moduli relate the out-of-plane shear stresses to the associated strain components only if the latter are assumed constant along the thickness, and thus equal to the average values $\bar{\gamma}_{zx}, \bar{\gamma}_{yz}$. A gross approximation, this, that may be overcome by extending the Jourawsky equilibrium considerations introduced for beams, to the plate realm. The actual treatise is however both complicated and, still, inexact[16].

In the case of homogeneous, linearly elastic plate material, an energetically consistent material law for the out-of-plane shear may be obtained by scaling the pointwise stress/strain relation[17]

$$\begin{bmatrix} \tau_{zx} \\ \tau_{yz} \end{bmatrix} = \underline{\underline{\mathrm{D}}}_{\gamma} \begin{bmatrix} \gamma_{zx} \\ \gamma_{yz} \end{bmatrix}, \tag{1.70}$$

by a 6/5 factor, thus obtaining the emended, average out-of-plane shear stress components

$$\begin{bmatrix} \bar{\tau}_{zx} \\ \bar{\tau}_{yz} \end{bmatrix} = \underbrace{\left(\frac{6}{5} \underline{\underline{\mathrm{D}}}_{\gamma} \right)}_{\bar{\underline{\underline{\mathrm{D}}}}_{\gamma}} \begin{bmatrix} \bar{\gamma}_{zx} \\ \bar{\gamma}_{yz} \end{bmatrix}, \tag{1.71}$$

Such relation is energetically consistent in the sense of the following equality

$$\frac{1}{2} \int_z \gamma_{zx} \tau_{zx} + \gamma_{yz} \tau_{yz} dz = \frac{1}{2} \begin{bmatrix} \bar{\gamma}_{zx} \\ \bar{\gamma}_{yz} \end{bmatrix}^{\top} \begin{bmatrix} \bar{\tau}_{zx} \\ \bar{\tau}_{yz} \end{bmatrix} h \tag{1.72}$$

$$= \frac{1}{2} \begin{bmatrix} \bar{\gamma}_{zx} \\ \bar{\gamma}_{yz} \end{bmatrix}^{\top} \bar{\underline{\underline{\mathrm{D}}}}_{\gamma} \begin{bmatrix} \bar{\gamma}_{zx} \\ \bar{\gamma}_{yz} \end{bmatrix} h. \tag{1.73}$$

[16] See e.g. MSC.Marc 2013.1 Documentation, Vol. A, pp. 433-436

[17] As an example, the definition for $\underline{\underline{\mathrm{D}}}_{\gamma}$ in the case of an orthotropic material whose out-of-plane shear moduli are G_{z1} and G_{2z} is

$$\underline{\underline{\mathrm{D}}}_{\gamma} = \begin{bmatrix} n^2 G_{z1} + m^2 G_{2z} & mnG_{z1} - mnG_{2z} \\ mnG_{z1} - mnG_{2z} & m^2 G_{z1} + n^2 G_{2z} \end{bmatrix},$$

where $m = cos\,\alpha$, $n = sin\,\alpha$, and α is the angle between the first in-plane principal direction of ortotropy, namely 1, and the local x axis.

The definition of the $\underline{\underline{\bar{\mathrm{D}}}}_{\gamma}$ matrix for composite laminates, or in the case of nonlinear material behaviour, is Beyond the Scope of the Present Contribution (BSPC).

1.3.5 The element stiffness matrix.

In this paragraph, the elastic behaviour of the finite element under scrutiny is derived.

The element is considered in its deformed configuration, being

$$\underline{\mathrm{d}}^{\top} = \begin{bmatrix} \underline{\mathrm{u}}^{\top} & \underline{\mathrm{v}}^{\top} & \underline{\mathrm{w}}^{\top} & \underline{\theta}^{\top} & \underline{\varphi}^{\top} \end{bmatrix} \tag{1.74}$$

the Degree of Freedom (DOF) vector associated with such condition.

A virtual displacement field perturbs such deformed configuration; as usual, those virtual displacements are infinitesimal, they do occur while time is held constant, and, being otherwise arbitrary, they respect the existing kinematic constraints.

Whilst, in fact, no external constrains are applied to the element, the motion of the pertaining material points is prescribed based on a) the assumed plate kinematics, and b) on the bilinear, isoparametric interpolation laws that propagate the generalized nodal displacements $\delta\,\underline{\mathrm{d}}$ towards the quadrilateral's interior.

Since the element is supposed to elastically react to such deformed configuration, a set of external actions

$$\underline{\mathrm{F}}^{\top} = \begin{bmatrix} \underline{\mathrm{U}}^{\top} & \underline{\mathrm{V}}^{\top} & \underline{\mathrm{W}}^{\top} & \underline{\Theta}^{\top} & \underline{\Phi}^{\top} \end{bmatrix} \tag{1.75}$$

is applied at nodes[18] – one each DOF, that equilibrate the stretched element reactions.

The nature of each $\underline{\mathrm{F}}$ generalized force component is defined based on the nature of the associated generalized displacement, such that the overall virtual work they perform on any $\delta\,\underline{\mathrm{d}}$ motion is

$$\delta Q_{\mathrm{e}} = \delta\,\underline{\mathrm{d}}^{\top}\,\underline{\mathrm{F}}\,. \tag{1.76}$$

The in-plane stress components that are induced by the $\underline{\mathrm{d}}$ generalized displacements equal

$$\underline{\sigma} \;=\; \underline{\underline{\mathrm{D}}}\,(z)\,\big(\,\underline{\underline{\mathrm{B}}}_{0}(\xi,\eta) + \underline{\underline{\mathrm{B}}}_{1}(\xi,\eta)z\big)\;\underline{\mathrm{d}} \tag{1.77}$$

[18] There is no lack of generality in assuming the equilibrating external actions applied at DOFs only, as discussed in Par. XXX below.

according to the previous paragraphs. They perform (volumic) internal work on the

$$\delta \underline{\epsilon} = \left(\underline{\underline{\mathrm{B}}}_0(\xi,\eta) + \underline{\underline{\mathrm{B}}}_1(\xi,\eta) z \right) \delta \underline{\mathrm{d}} \tag{1.78}$$

virtual elongations.

The associate internal virtual work may be derived by integration along the element volume, i.e. along the thickness, and along the quadrilateral portion of reference surface that pertains to the element. We thus obtain a first contribution to the overall internal virtual work

$$\begin{aligned}
\delta Q_{\mathrm{i}}^{\sigma} &= \iint_{\mathcal{A}} \int_h \delta \underline{\epsilon}^{\top} \underline{\sigma} \, dz d\mathcal{A} \\
&= \iint_{\mathcal{A}} \int_h \left(\left(\underline{\underline{\mathrm{B}}}_0 + \underline{\underline{\mathrm{B}}}_1 z \right) \delta \underline{\mathrm{d}} \right)^{\top} \underline{\underline{\mathrm{D}}} \left(\underline{\underline{\mathrm{B}}}_0 + \underline{\underline{\mathrm{B}}}_1 z \right) \underline{\mathrm{d}} \, dz d\mathcal{A} \\
&= \delta \underline{\mathrm{d}}^{\top} \left[\iint_{\mathcal{A}} \int_h \left(\underline{\underline{\mathrm{B}}}_0^{\top} + \underline{\underline{\mathrm{B}}}_1^{\top} z \right) \underline{\underline{\mathrm{D}}} \left(\underline{\underline{\mathrm{B}}}_0 + \underline{\underline{\mathrm{B}}}_1 z \right) dz d\mathcal{A} \right] \underline{\mathrm{d}} \\
&= \delta \underline{\mathrm{d}}^{\top} \underline{\underline{\mathrm{K}}}_{\sigma} \underline{\mathrm{d}}
\end{aligned} \tag{1.79}$$

Integration along i) the reference surface, and ii) along the thickness is numerically performed through potentially distinct quadrature rules; in particular, contributions are collected along the surface according to the two points per axis (four points overall) Gaussian quadrature formula introduced in Par. 1.1.2, whilst a (composite) Simpson rule is applied in z, being each material layer sampled at its outer and middle points.

The two points per axis quadrature rule is the lowest order rule that returns an exact integral evaluation in the case of *distortion-free*[19] elements, i.e. planar elements whose peculiar (parallelogram) shape also determines a linear (vs. bilinear) isoparametric mapping. Since the associated Jacobian matrix is constant with respect to ξ, η, the $\underline{\underline{\mathrm{L}}}$ matrix defined in1.60 linearly varies with such isoparametric coordinates, and so do the $\underline{\underline{\mathrm{B}}}_0$, $\underline{\underline{\mathrm{B}}}_1$ matrices. The integrand of Eqn. 1.79 is thus a quadratic function of the ξ, η integration variables, as the Jacobian matrix determinant that scales the physical and the natural infinitesimal areas is also constant XXX.

[19] Many distinct definitions are associated to the element distortion concept, being the one reported relevant for the specific dissertation passage.

A second contribution, which is due to the out-of-plane shear components, may be obtained with similar considerations, and based on Eqns. 1.69 and 1.73; such contribution may be cast as

$$\begin{aligned}\delta Q_{\mathrm{i}}^{\gamma} &= \iint_{\mathcal{A}} \int_{h} \delta \underline{\bar{\gamma}}^{\top} \underline{\bar{\tau}} \, dz d\mathcal{A} \\ &= \delta \underline{\mathrm{d}}^{\top} \left[h \iint_{\mathcal{A}} \underline{\underline{\mathrm{B}}}_{\gamma}^{\top} \underline{\underline{\bar{\mathrm{D}}}}_{\gamma} \underline{\underline{\mathrm{B}}}_{\gamma} d\mathcal{A} \right] \underline{\mathrm{d}} \\ &= \delta \underline{\mathrm{d}}^{\top} \underline{\underline{\mathrm{K}}}_{\gamma} \underline{\mathrm{d}} \,. \end{aligned} \tag{1.80}$$

The overall internal work is thus

$$\begin{aligned}\delta Q_{\mathrm{i}} &= \delta Q_{\mathrm{i}}^{\sigma} + \delta Q_{\mathrm{i}}^{\gamma} \\ &= \delta \underline{\mathrm{d}}^{\top} \left(\underline{\underline{\mathrm{K}}}_{\sigma} + \underline{\underline{\mathrm{K}}}_{\gamma} \right) \underline{\mathrm{d}} \\ &= \delta \underline{\mathrm{d}}^{\top} \underline{\underline{\mathrm{K}}} \, \underline{\mathrm{d}} \,. \end{aligned} \tag{1.81}$$

The principle of virtual works states that the external and the internal virtual works are equal for a general virtual displacement $\delta \underline{\mathrm{d}}$, namely

$$\delta \underline{\mathrm{d}}^{\top} \underline{\mathrm{F}} = \delta Q_{\mathrm{e}} = \delta Q_{\mathrm{i}} = \delta \underline{\mathrm{d}}^{\top} \underline{\underline{\mathrm{K}}} \, \underline{\mathrm{d}} \,, \quad \forall \delta \underline{\mathrm{d}} \,, \tag{1.82}$$

if and only if the applied external actions $\underline{\mathrm{F}}$ are in equilibrium with the elastic reactions due to the displacements $\underline{\mathrm{d}}$; the following equality thus holds

$$\underline{\mathrm{F}} = \underline{\underline{\mathrm{K}}} \, \underline{\mathrm{d}} \,; \tag{1.83}$$

the $\underline{\underline{\mathrm{K}}}$ *stiffness matrix* relates a deformed element configuration, which is defined the the generalized displacement vector $\underline{\mathrm{d}}$, with the $\underline{\mathrm{F}}$ generalized forces that have to be applied at the element nodes to keep the element in such a stretched state.

1.3.6 The shear locking flaw

Figure 1.5 rationalizes the shear locking phenomenon that plagues the bilinear isoparametric element in its mimicking the pure bending deformation modes, with both in-plane and out-of-plane constant curvature.

An ingenious sampling and interpolation technique has been developed in [2] that overcomes the locking effect due to the spurious transverse shear strain that develops when the element is subject to out-of-plane bending. Such technique, however, does not correct the element behaviour with respect to in-plane bending.

Eqn. 1.69 is employed in obtaining the tranverse shear strain components $\bar{\gamma}_{zx}$ and $\bar{\gamma}_{yz}$ at the edge midpoints; the edge-aligned component $\bar{\gamma}_{z\hat{ij}}$ is derived by projection along the $\hat{ij}$ direction, whereas the orthogonal component is neglected.

Figure 1.6a evidences that a null spurious tranverse shear is measured at the midpoint of the 12 and of the 41 edges when a constant, out-of-plane curvature is locally enforced that develops along the $\hat{12}$ and the $\hat{41}$ directions, respectively. Such property holds for all edges.

In Figure 1.6b, a differential out-of-plane displacement is added to the initial pure bending configuration of Fig. 1.6a, and in the absence of further rotations at nodes; a proper (vs. spurious) tranverse shear strain field is thus induced in the element, that the sampling scheme should properly evaluate.

The edge aligned, transverse shear components sampled at the side midpoints are then assigned to the whole edge, and in particular to both its extremal nodes.

As shown in Figure 1.6b (and in the related enlarged view), two independent transverse shear components $\bar{\gamma}_{z\hat{12}}$ and $\bar{\gamma}_{z\hat{41}}$ are associated to the n1 node, which is taken as an example.

A vector is uniquely determined, whose projections on the $\hat{12}$ and $\hat{41}$ directions coincide with the associated transverse shear components; the components of such vector with respect to the x, y axes define the $\bar{\gamma}_{zx,\mathrm{n1}}$ and $\bar{\gamma}_{yz,\mathrm{n1}}$ tranverse shear terms at the n1 node.

Such procedure is repeated for all the element vertices; the obtained nodal values for the transverse shear components are then interpolated to the element interior, according to the costumary bilinear scheme.

Due to the peculiarity of the initial sampling points, the obtained tranverse shear strain field is amended with respect to the spurious

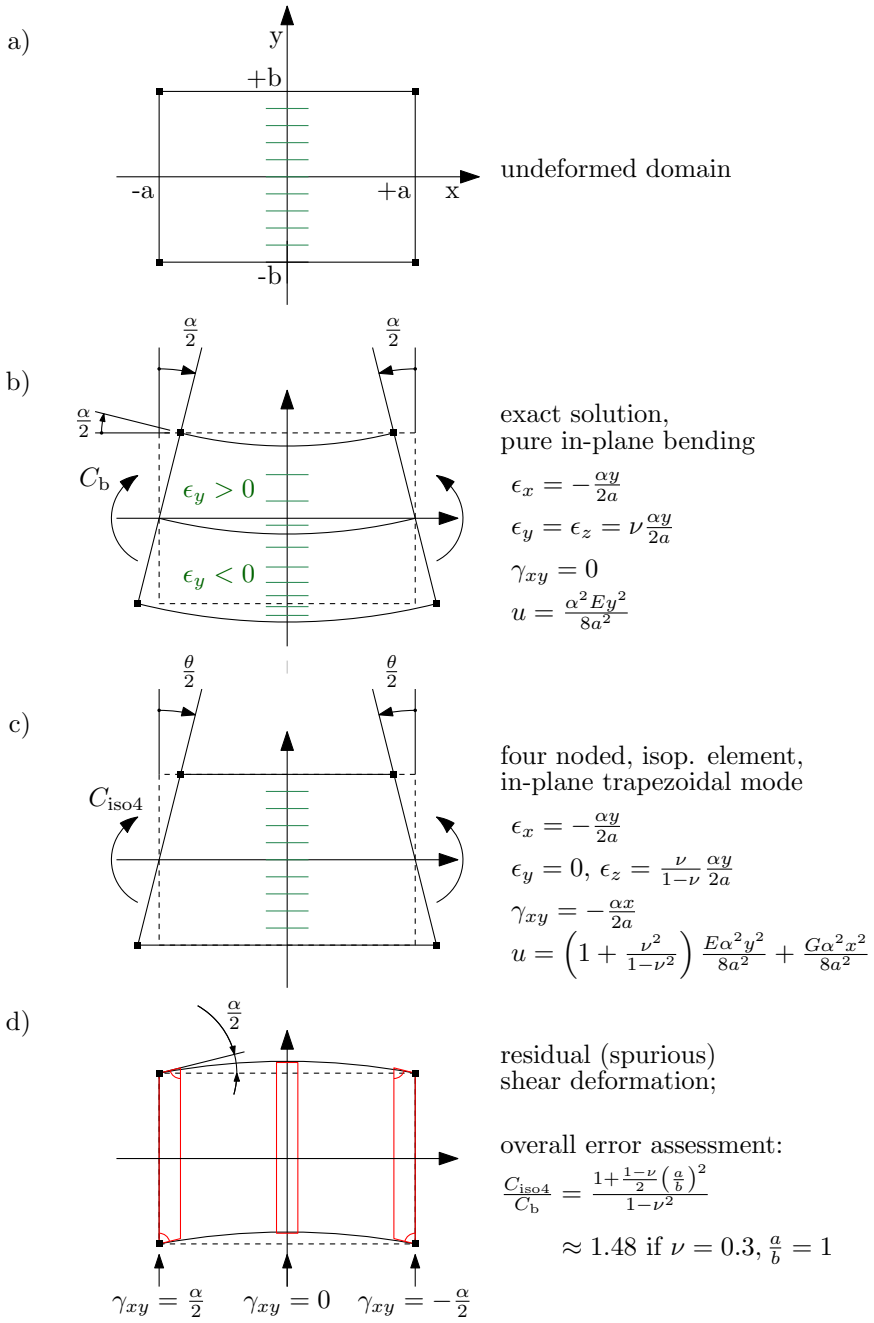

Figure 1.5: Rationalization of the shear locking phenomenon.

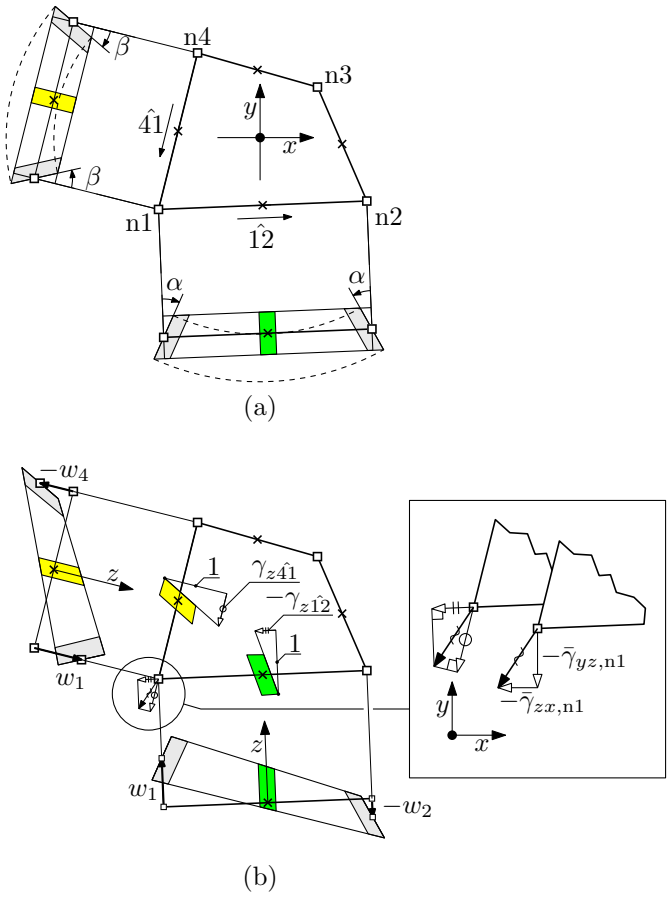

Figure 1.6: A tranverse shear sampling technique employed in the four-noded isoparametric element for preventing shear locking in the out-of-plane plate bending.

contribution that previously led to the shear locking effect; the usual quadrature scheme may now be employed.

Equation 1.69 still formalizes the passage from nodal DOFs to the out-of-plane shear field, since the procedure described in the present paragraph may be easily cast in the form of a revised $\underline{\underline{\mathrm{B}}}_{\gamma}$ matrix.

1.4 Joining elements into structures.

1.4.1 Displacement and rotation field continuity

Displacement and rotation fields are continuous at the isoparametric quadrilateral inter-element interfaces; they are in fact continuous at nodes since the associated nodal DOFs are shared by adjacent elements, and the field interpolations that occur within each quadrilateral domain a) they both reduce to the same linear relation along the shared edge, and b) they are performed in the absence of any contributions related to unshared nodes.

1.4.2 Expressing the element stiffness matrix in terms of global DOFs

As seen in Par. 1.3.5, the stiffness matrix of each j-th element defines the elastic relation between the associated generalized forces and displacements, i.e.

$$\underline{\mathrm{F}}_{\mathrm{e}j} = \underline{\underline{\mathrm{K}}}_{\mathrm{e}j}\,\underline{\mathrm{d}}_{\mathrm{e}j} \tag{1.84}$$

where the DOFs definition is local with respect to the element under scrutiny.

In order to investigate the mutual interaction between elements in a structure, a common set of *global* DOFs is required; in particular, generalized displacement DOFs are defined at each l-th global node, i.e., for nodes interacting with the shell element formulation under scrutiny,

$$\underline{\mathrm{d}}_{\mathrm{g}l} = \begin{bmatrix} u_{\mathrm{g}l} \\ v_{\mathrm{g}l} \\ w_{\mathrm{g}l} \\ \theta_{\mathrm{g}l} \\ \varphi_{\mathrm{g}l} \\ \psi_{\mathrm{g}l} \end{bmatrix} . \tag{1.85}$$

The global reference system $\mathrm{O}XYZ$ is typically employed in projecting nodal vector components. However, each l-th global node may be supplied with a specific reference system, whose unit vectors are $\hat{\imath}_{\mathrm{g}l}, \hat{\jmath}_{\mathrm{g}l}, \hat{k}_{\mathrm{g}l}$, thus permitting the employment of non uniformly aligned (e.g. cylindrical) global reference systems.

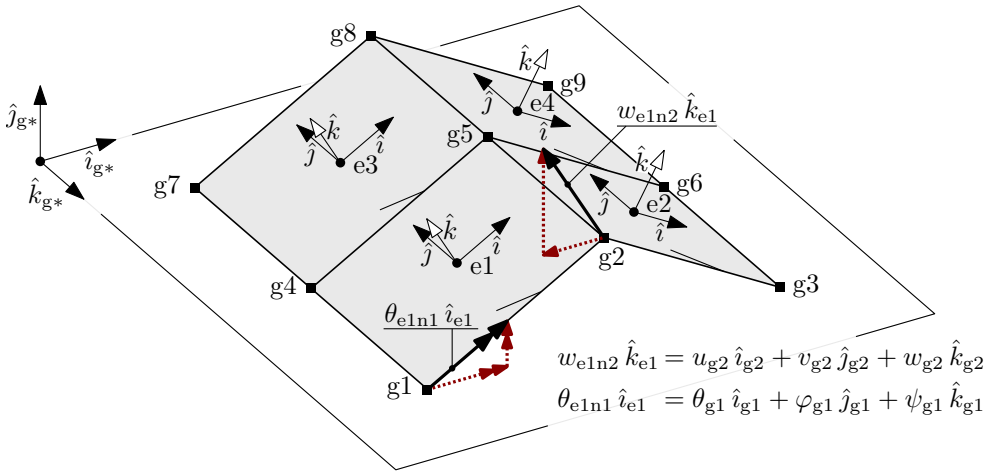

Figure 1.7: A simple four-element, roof-like structure employed in discussing the assembly procedures. The elements are square, thick plates whose angle with respect to the global XY plane is 30°

Those nodal degrees of freedom may be collected in a global DOFs vector

$$\underline{\mathrm{d}}_{\mathrm{g}}^{\top} = \left[\underline{\mathrm{d}}_{\mathrm{g}1}^{\top} \quad \underline{\mathrm{d}}_{\mathrm{g}2}^{\top} \quad \dots \quad \underline{\mathrm{d}}_{\mathrm{g}l}^{\top} \quad \dots \quad \underline{\mathrm{d}}_{\mathrm{g}n}^{\top}\right] \tag{1.86}$$

that parametrically defines any deformed configuration of the structure.

Analogously, a global, external (generalized[20]) forces vector may be defined, that assumes the form

$$\underline{\mathrm{F}}_{\mathrm{g}}^{\top} = \left[\underline{\mathrm{F}}_{\mathrm{g}1}^{\top} \quad \underline{\mathrm{F}}_{\mathrm{g}2}^{\top} \quad \dots \quad \underline{\mathrm{F}}_{\mathrm{g}l}^{\top} \quad \dots \quad \underline{\mathrm{F}}_{\mathrm{g}n}^{\top}\right]; \tag{1.87}$$

since external constraints are expected to be applied to the structure DOFs, the following vector of reaction forces

$$\underline{\mathrm{R}}_{\mathrm{g}}^{\top} = \left[\underline{\mathrm{R}}_{\mathrm{g}1}^{\top} \quad \underline{\mathrm{R}}_{\mathrm{g}2}^{\top} \quad \dots \quad \underline{\mathrm{R}}_{\mathrm{g}l}^{\top} \quad \dots \quad \underline{\mathrm{R}}_{\mathrm{g}n}^{\top}\right] \tag{1.88}$$

is introduced.

[20] Unless otherwise specified, the *displacement* and *force* terms refer to the DOFs, and the suitable actions that perform work with their variation, respectively. They are in fact *generalized* forces and displacements.

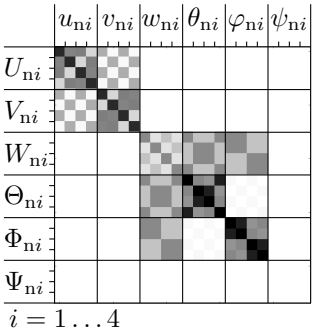

Figure 1.8: A representation of the stiffness matrix terms for each element in the example structure; the term magnitude is represented through a linear grayscale, spanning from zero (white) to the peak value (black).

The simple four element, roof-like structure of Fig. 1.7 is employed in the following to discuss the procedure that derives the elastic response characterization for the structure from its elemental counterparts.

The structure comprises nine nodes, whose location in space is defined according to a global reference system OXYZ, see Table XXX. The structure is composed by four, identical, four noded isoparametric shell elements, whose formulation is described in the preceding section 1.3.

A grayscale, normalized representation of the element stiffness matrix is shown in Figure 1.8.

XXX

The $\underline{\underline{\mathrm{P}}}_{ej}$ mapping matrix is orthogonal...

1.5 Constraints.

XXX

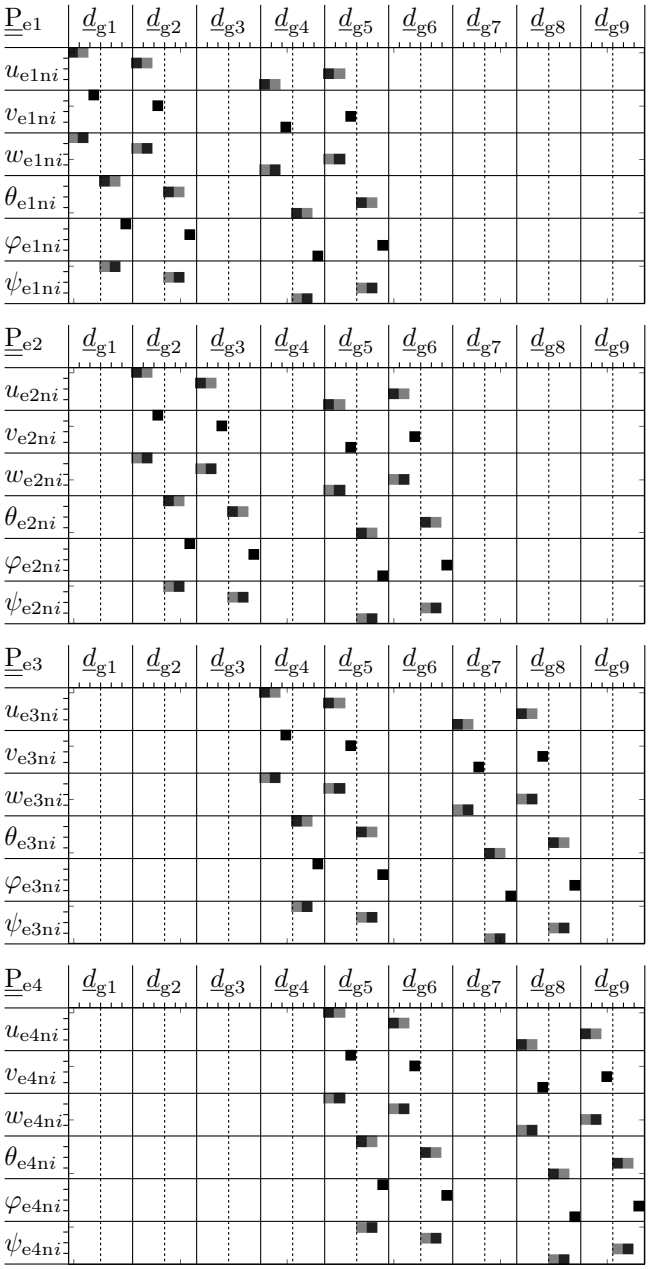

Figure 1.9: A grayscale representation of the terms of the four $\underline{\underline{\mathrm{P}}}_{\mathrm{e}j}$ mapping matrices associated the elements of Fig. 1.7.

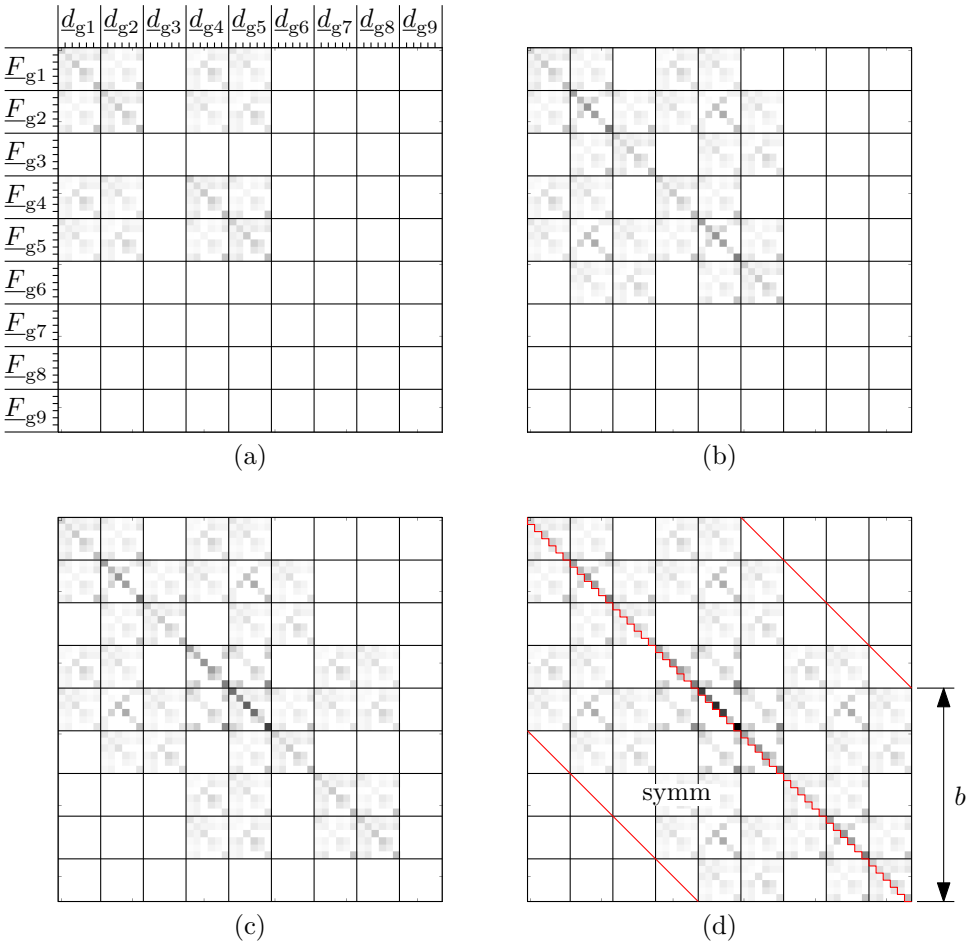

Figure 1.10: Graphical representation of the assembly steps for the stiffness matrix of the Fig. 1.7 structure. The zero-initialized form for the matrix that precedes the (a) step is omitted.

Bibliography

[1] C. Hua, "An inverse transformation for quadrilateral isoparametric elements: analysis and application," *Finite elements in analysis and design*, vol. 7, no. 2, pp. 159–166, 1990.

[2] T. J. Hughes and T. Tezduyar, "Finite elements based upon mindlin plate theory with particular reference to the four-node bilinear isoparametric element," *Journal of applied mechanics*, vol. 48, no. 3, pp. 587–596, 1981.